

## Influence of Illumination on Color based Potato Defect Detection

Amrinder Singh Brar<sup>1\*</sup> & Kawaljeet Singh<sup>2</sup>

<sup>1</sup>Department of Computer Science and Engineering, <sup>2</sup>Computer Centre, Punjabi University, Patiala 147 002, Punjab, India

Received 06 July 2022; revised 12 June 2023; accepted 09 July 2023

The global vegetable market demands rigorous quality analysis of potato crops to define their reasonable market price. Highly accurate machine learning-based automated potato defect detection systems are necessary for this rising global market. On the other hand, artificial illuminating lamps used in these machine learning systems are decisive in determining their defect detection accuracy. Artificial illuminating lamps used in these machine learning systems should provide a perception of color that is as similar as possible to natural potato color. This paper analysed potato skin color measuring accuracy of seven different illumination lamps (L01 to L07). The analysis used ten potato samples with various defects, including one healthy potato. Experimental results proved that the lowest  $\Delta E^*$  was obtained when the Compact Fluorescent lamp 45W, 6500 Correlated Color Temperature (CCT) (L1) was used as an illuminating lamp. The proposed experimental study will help to develop machine learning methodologies in future research by generating higher accuracies for potato defect detection using an L01-type illuminating lamp.

**Keywords:** Computer vision, Food quality, Image acquisition, Measurement and instrumentation, Standardization

### Introduction

Potato is one of the most popular tubercles cultivated in 80% of countries, with worldwide production exceeding 300 million tons per year.<sup>1</sup> Potato defects like a common scab, crack, late blight, dry rot, powdery scab, early blight, soft rot and greening can be identified based on the appearance of potato skin. Thus the visual appearance of the potato crop influences its quality and, ultimately, the selling price.<sup>2</sup> Defect detection in agricultural products like potatoes is a vital task which influences the efficiency of farming as well as the economy of developing countries.<sup>3</sup> Initially quality of the potato crop was determined visually with the help of manual quality inspectors. During this process, human inspectors visually inspect and classify each tuber using the naked eye. However, as the technology evolved, many computer vision-based defect detection and quality control systems were developed in the prior art.<sup>4-10</sup> The computer vision-based defect detection helped to enhance the frequency of monitoring the quality of fruit and vegetables, which contributes in maintaining demand and supply of agricultural products.<sup>11</sup> The great diversity of potato external defects with varying textures and color emphasizes the importance of the accuracy of illuminating lamps

used in the computer vision system. An accurate illumination system helps maximise the accuracy of the defect detection system, thus enhancing the quality of final results.<sup>12</sup>

The potato peel color is one of the decisive factors in determining if potato tuber is defective or healthy; the factors influencing potato color measurement must be considered in developing computer vision systems. The color perception of the object is directly affected by the type of illumination used to measure the object's colour. Different illuminating lamps are used in the different state-of-the-art potato defect detection systems. Barnes *et al.* used daylight bulbs as an illuminating light source to develop a computer vision-based method to detect visual blemishes in potatoes.<sup>5</sup> In another prior artwork, Razmjoooy *et al.* used two fluorescent lights to develop a machine vision-based potato defect detection and size sorting system.<sup>6</sup> Oppenheim & Shani acquired images of 400 contaminated potatoes under uncontrolled illumination conditions like commercial lamps used in the present study.<sup>13</sup> These were further utilized for potato defect classification using convolution neural networks. In another prior artwork, two Philips, 6400K, 18W fluorescent lamps were used to develop a machine vision-based potato image acquisition system. In this methodology potato quality grading system was proposed based on machine vision and 3d shape analysis.<sup>14</sup> Ming *et al.* utilized a ring Light-Emitting

\*Author for Correspondence  
E-mail: amrinder.web@gmail.com

Diode (LED) lamp for illuminating samples from the top to detect sprouting in potatoes. In this methodology optical measuring instrument using a Charge-Coupled Device (CCD) camera and LED lamp was proposed.<sup>15</sup> In another prior art, an LED lamp illuminating source was utilized during the image acquisition phase of weakly-supervised learning-based potato defect segmentation methodology.<sup>2</sup> Marino *et al.* proposed an unsupervised deep domain adaptation method for classifying potato defects. This methodology utilised LED panels as illuminating lamps during the image acquisition phase.<sup>16</sup> Si *et al.* developed an image acquisition system using a CCD camera (FL3-GE-13S2C-CS, RoHS 1.3 MP Color Flea3 GigE Camera, Point Grey Research Inc., Richmond, BC, Canada) with a 2.8–8 mm lens and fluorescent lamps (75 to 90 Lux) for automated potato tuber shape evaluation.<sup>17</sup> In all the potato defect detection methods mentioned above, illuminating lamps were selected purely based on their popularity in prior art studies. No scientific study is available where the best illuminating lamps for potato defect detection have been analysed and authorized. This motivated us to perform the present study. In another similar prior study, the influence of illuminating lamps on the visual characterization of banana ripening stages was performed.<sup>12</sup> In this study classification of seven banana ripening stages (subclasses C1 to C7 of Von Loesecke) using nine different commercial lamps was compared. It was concluded that Double envelope incandescent tube halogen 1000W illuminating lamp performed most accurate classification of banana ripening stages. This study was merely focused on commercial lamps and was based on visual analysis. Thus this study is not applicable to lighting used in image acquisition systems developed for computer vision based fruit and vegetable defect detection devices. Also, common photography lighting or controlled lighting used in the image acquisition systems were not analysed in the above study. Thus there is clear research gap which demands analyses of various controlled and commercial lighting systems used for image acquisition. So that standardized lighting solutions can be developed for future studies. Standardizing single illuminating lamp type for defect detection of each fruit or vegetable type is not feasible. Thus, analyses of illuminating lamps for each fruit and vegetable type are needed. This motivated us to perform analyses of potato color measuring accuracy using seven different types of illumination lamps (L01 to L07) in the proposed study.

## Materials and Methods

### Potato Sample Selection

A total of 10 potato samples were obtained from the produce of farms in Punjab, India, available in the local vegetable market. The variety of potatoes used in the proposed experiment was Kufri Jyoti. Of these ten potato samples, nine were defective, and one was healthy. The defective potatoes include potatoes infected by diseases like common scabs, crack, late blight, dry rot, powdery scab, early blight, soft rot and greening. The use of these potato defects in previous Computer Vision (CV) based defect detection research motivated us to include them in the present study. The purpose of taking ten unique potato samples was to study the influence of various illuminating lamps on measuring the color of each defective and healthy potato. The images of each potato sample used in the present study are visualized in Fig. 1(a).

### Illuminating Lamps Selection

The object's colour is directly influenced by the illumination source under which it is visualized.<sup>18</sup> Thus,

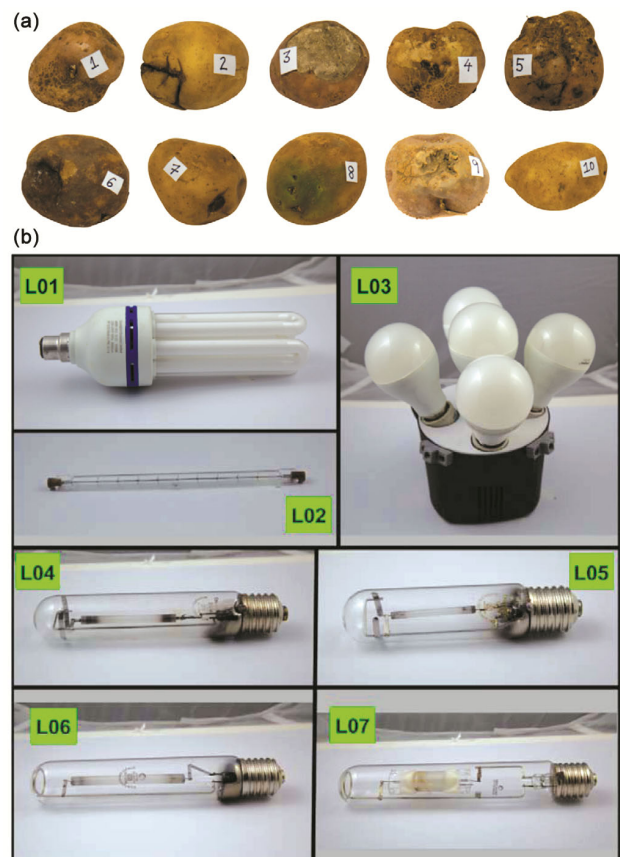


Fig. 1 — Images of each: (a) potato sample (01 to 10) and; (b) illuminating lamp (L01 to L07) used in the proposed methodology

the type of illumination used in color-based potato defect detection devices highly influences the prediction accuracy. The present study analysed three continuous photography and four commercial lights based on their accuracy in measuring the color of defective and healthy potatoes. Continuous photography lights were selected based on their popularity in computer vision applications. On the other hand, commercial lights were chosen due to their intense utilization in food grading and industrial environments.<sup>12</sup> The commercial lights were analysed since various CV-based food grading devices operate under lights used in the surrounding environment instead of specialised illumination. The illumination lamp types used in the present study are elaborated in Table 1. The first column describes the unique code applied to each illuminating lamp type, the second column represents the lamp type, the lamp category is described in the third column, and the last column displays the Correlated Color Temperature (CCT) in Kelvin of each lamp. The images of each illuminating lamp used in the proposed methodology are visualized in Fig. 1(b).

#### Experimental Setup for Analysing Lamps

The distance-based color-measuring device was developed to investigate the accuracy of potato color measured under seven different illuminating lamps. Distance-based color measuring device initially measures potatoes' colour using a digital camera. After this, measured color values are provided to the calibrating unit. The calibrating unit generates accurate color values using a trained ensemble-based regression algorithm.

CIELab system is a standardized color measuring system defined by the International Commission of Illumination (CIE).<sup>19</sup> In CIELab, lightness is represented by  $L^*$ , red/green coordinates are represented by  $a^*$  and yellow/blue coordinates are represented by  $b^*$ .<sup>20</sup> CIELab system measurements are perceived to be very similar to human color perception and thus CIELab system is frequently used color space in the prior art agriculture sector computer

vision applications.<sup>21</sup> This motivated us to use the CIELab system as a color-measuring system in the present study.<sup>22,23</sup> In the CIELab space, when two colors are compared, the total color difference ( $\Delta E^*$ ) introduced by International Commission on Illumination (CIE) is defined as:

$$\Delta E^* = \sqrt{\Delta L^{*2} + \Delta a^{*2} + \Delta b^{*2}} \quad \dots (1)$$

where,  $\Delta E^*$  is a color difference,  $\Delta L^*$  is a difference in the lightness value of two colors,  $\Delta a^*$  is a difference in red/green coordinates and  $\Delta b^*$  is a difference in the yellow/blue coordinates of the two colors. The lower value of  $\Delta E^*$  is considered as a lesser difference in color perception of two colors.

#### Methodology Diagram

The methodology of developing an experimental device to assess the influence of different illuminating lamps on color-based potato defect detection methods is visualized in Fig. 2. In the proposed methodology, initially, the color of nine defective and one healthy potato sample is measured using seven different lighting sources ( $L01$  to  $L07$ ). Since Red Green Blue (RGB) color values of potato samples captured by the digital camera depend on the device used and the environment under which the experiment is performed.<sup>24</sup> Thus, a specially assembled distance-based color measuring device was used to calibrate inaccurate color values measured by a digital camera and provide accurate device-independent color values of potato samples. The RGB color values captured by the digital camera are provided to the color calibrating unit, which converts them into CIELab color space. The converted CIELab space color values ( $L^*, a^*$  and  $b^*$ ) are provided as input to a pre-trained ensemble-based regression algorithm to predict accurate device-independent color values of potato samples. In the next step, X-Rite Spectro-colorimeter with D65 luminance is used to measure accurate color values of same potato samples in CIELAB color space ( $CIE L^* a^* b^*$ ). The Spectrocolorimeter must touch the

Table 1 — Illuminating lamp types used in measuring color values of potato samples

Code	Lamp Type	Category	CCT(K)
L01	Compact fluorescent lamp Crompton Greaves 45W(4U)-DF/65	Continues Photography Lights	6500
L02	Double envelope Simplex platinum incandescent tube halogen 1000W	Continues Photography Lights	3600
L03	Lighting fixture Simplex Pro HD LED 5 125 W	Continues Photography Lights	6500
L04	High-pressure tube sodium steam Crompton Greaves 250 W IS:9974	Commercial Lights	2000
L05	High-pressure tube sodium steam Crompton Greaves 150 W IS:9974	Commercial Lights	2000
L06	High-pressure tube sodium steam Crompton Greaves 400 W IS:9974	Commercial Lights	2000
L07	High-pressure tube Metal Halide Crompton Greaves 400 W MH-S/T	Commercial Lights	4100

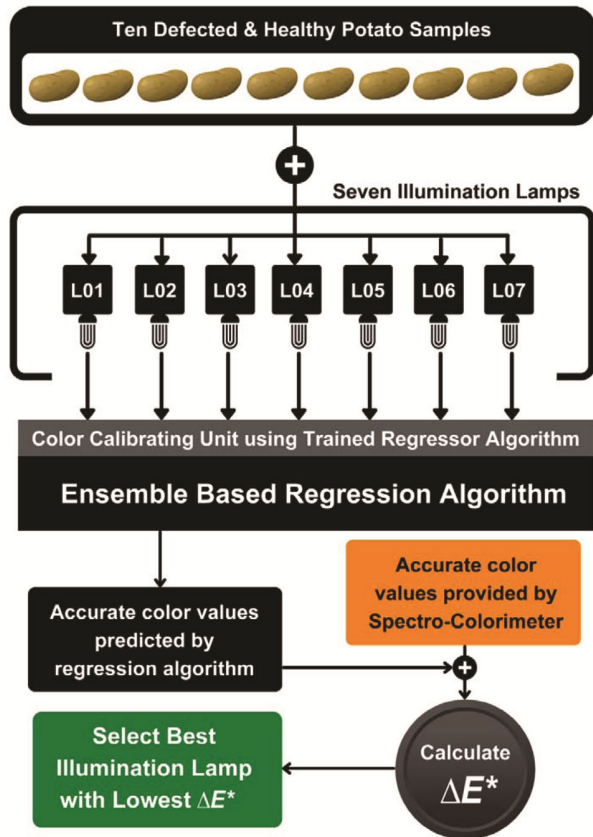


Fig. 2 — Flow diagram representing the study of the influence of illumination on color-based potato defect detection

potato sample to measure accurate color values. Thus the color values measured by X-Rite Spectrocolorimeter are device and environment independent. So they are considered as standard color values to find color difference  $\Delta E^*$  for each illuminating lamp (L01 to L07) in the present study. In the last step, color difference  $\Delta E^*$  values are calculated for each illuminating lamp (L01 to L07) using color values provided by the calibrating unit and X-Rite Spectrocolorimeter. The illuminating lamp with the lowest average color difference  $\Delta E^*$  is considered the best lighting source for image acquisition in color-based potato defect detection methods.

**Color Measurement under Illuminating Lamps**

The experimental setup for distance-based color measuring of potato samples illuminated by lamps placed right above the samples is displayed in Fig. 3(a). The illuminating lamp is placed on a supporting arc such that the angle between the light emitted by the lamp and the digital camera is  $45^\circ$  following optical geometry of visualization normal/ $45^\circ$  ( $0^\circ:45^\circ$ ). Optical geometry of visualization

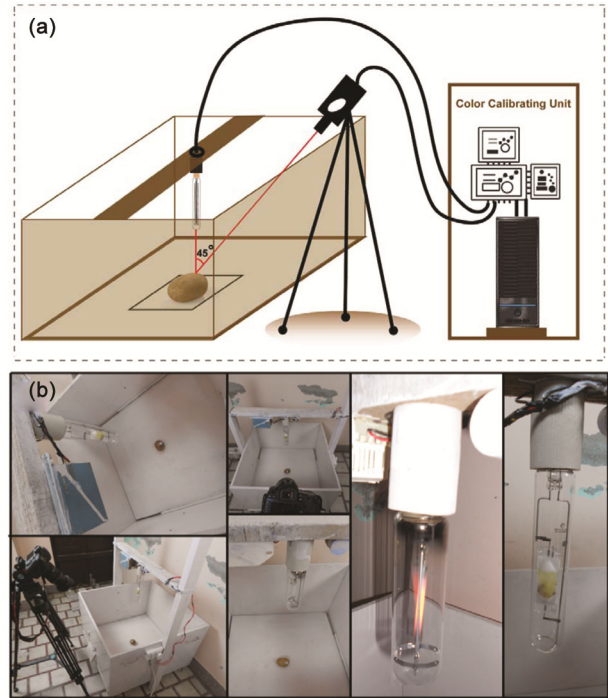


Fig. 3 — (a) 3D diagram representing experimental setup for distance-based color measuring of potato samples; (b) Laboratory images of the experimental setup used to perform proposed experimental methodology

normal helps enhance color or measuring accuracy by minimizing specular reflection errors generated by illuminating light sources on the target. The potato sample is placed at the centre of the base of the color measuring unit. Canon EOS 5D Mark III digital camera with EF24-105mm f/4L IS USM lens was used in the present methodology. The camera exposure was set to an aperture value of f/5.6, a shutter speed of 1/160 sec, a focal length of 97 mm, and an ISO of 100. No camera flash light was used while performing present study and experiments were performed in dark room with no external natural light. The distance of the camera lens centre from the ground was kept at 80cm, and the distance between the sample base and the light source base was held at 90cm. The interior of the color measuring unit is coated with white color for eliminating light reflections from the walls and dispersing light equally. The color calibrating unit is the Intel 7th Generation processor for executing an ensemble-based regressor algorithm for color calibration. The communication between the color calibrating unit and the color measuring unit is done with the help of data transfer wires. The color calibrating unit is responsible for providing device and environment

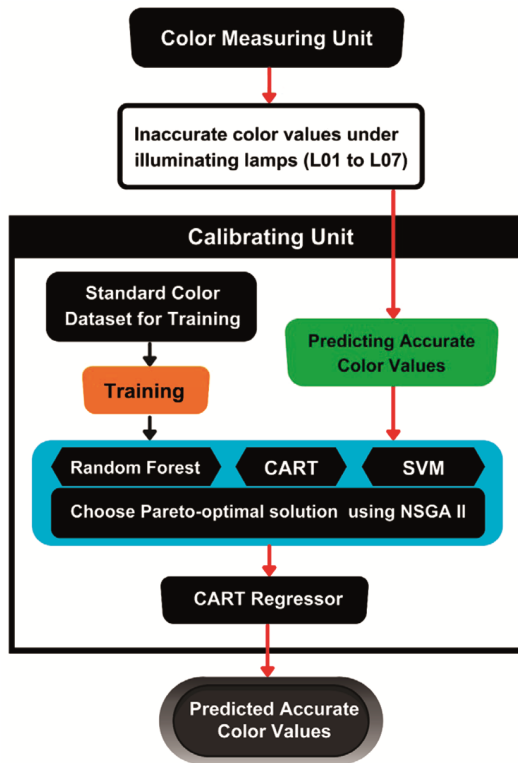


Fig. 4 — Flow diagram representing the process of color correction by color measuring unit

independent accurate color values measured by digital camera. The digital camera is supported by a tri-leg iron supporting stand (tripod), and the illuminating lamp is held on a wooden supporting arc. The laboratory images of the experimental setup of the proposed system are displayed in Fig. 3(b).

#### Color Calibrating Unit

The flow diagram in Fig. 4 summarizes the process of color correction by the color measuring unit. Initially, incorrect color values of potato samples provided by color measuring unit using illuminating lamps (*L01 to L07*) are provided to pre-trained ensemble-based regressor algorithm. Stacking as an ensemble is the methodology where predicted outputs of multiple base regressors are used as an input for a single meta-learner. In the proposed method, Random Forest (RF)<sup>25</sup>, Classification and Regression Tree (CART)<sup>26,27</sup> and Support Vector Machine (SVM)<sup>28–30</sup> were used as base regressors. In the final step, CART was used as a meta-regressor. Potato color values ( $L^*$ ,  $a^*$  and  $b^*$ ) predicted by base regressors along with original inaccurate color values are provided to Non-dominated Sorting Genetic Algorithm (NSGA-II) based model selection algorithm.<sup>31</sup> Model selection

Table 2 — Standard color values in CIELab color space of all potato samples

	Standard Color Measurements by Spectro-colorimeter		
	$L^*$	$a^*$	$b^*$
Common Scab	45.8	7.1	15.8
Crack	50.1	6.5	19.9
Late Blight	51.1	3.3	14.1
Dry rot	38.7	7.4	15.1
Powdery Scab	41.6	6.9	16.6
Early Blight S1	34.6	6.9	12.9
Soft Rot	37.6	7.6	16
Greening	40.6	1.2	13.6
Early Blight S2	38	4.4	13.5
Healthy	53.4	5.5	22.9

algorithm creates a Pareto-Optimal solution set which maximizes prediction accuracy. A Pareto-Optimal solution set consisting of predicted and original inaccurate color values is provided as input to the CART meta-regressor. Finally, accurate color values predicted by the CART meta-learner are provided as an output.

#### Results and Discussion

This section presents a comprehensive analysis of the influence of each illuminating lamp (*L01 to L07*) on color-based potato defect detection. Color values ( $L^*$ ,  $a^*$  and  $b^*$ ) of ten potato samples under each lighting source were used to calculate the average color difference  $\Delta E^*$  by using color values measured with X-Rite Spectro-colorimeter as standard. The dark room was used for analysing each illuminating lamp, and the environmental temperature was controlled to  $25 \pm 0.5^\circ\text{C}$  for mitigating any external factor or variation during analysis. Illuminance on the surface of potato samples was around 1000 lx after 30 minutes of illuminating lamp heating.

#### Analyses of Standard Color Measurements

This subsection elaborates on the standard color measurements the proposed methodology provides for all ten potato samples. X-Rite Spectro-colorimeter with D65 Luminance was utilized to retrieve accurate standard color values of potato samples. Standard colour values in the CIELab color space of all potato samples under test are tabulated in Table 2. Each row of the table represents standard color values obtained for each potato sample, and each column represents  $L^*$ ,  $a^*$  and  $b^*$  standard color values obtained for the respective sample.

Table 3 — CIELab color values obtained using different illuminating lamps (L01 to L07) used in the present study

		Common scab	Crack	Late Blight	Dry rot	Powdery scab	Early blight S1	Soft rot	Greening	Early blight S2	Healthy
L01	L*	47.425	47.425	50.875	37.967	41.925	35.538	37.967	40.329	37.967	53.400
	a*	6.983	6.225	2.250	7.159	7.159	7.159	7.159	1.200	5.667	5.500
	b*	17.292	17.292	14.100	15.460	17.292	13.358	15.460	14.007	14.007	21.778
L02	L*	47.425	47.425	50.875	37.967	47.425	35.538	37.967	40.329	37.967	50.875
	a*	7.159	7.159	3.667	7.159	7.159	7.159	7.159	1.200	3.667	5.667
	b*	17.292	17.292	14.007	15.460	17.292	13.358	15.460	15.460	14.007	21.778
L03	L*	41.925	47.425	50.875	37.967	41.925	35.538	37.967	39.300	39.300	50.875
	a*	6.225	5.667	3.667	7.159	6.225	6.983	7.159	1.200	5.667	5.500
	b*	14.007	17.292	14.007	15.460	15.460	13.358	15.460	13.358	13.358	21.778
L04	L*	50.875	42.356	50.875	42.356	37.967	37.967	37.967	42.356	40.329	53.400
	a*	6.983	5.667	3.667	6.983	7.159	7.159	7.159	2.250	5.667	5.500
	b*	21.778	19.900	14.100	16.140	17.292	14.007	17.292	14.007	14.007	21.778
L05	L*	47.425	47.425	50.875	40.329	42.356	35.538	37.967	42.356	37.967	53.400
	a*	7.159	7.159	3.667	7.159	6.983	7.159	7.159	1.200	6.225	5.667
	b*	17.292	17.292	14.100	15.460	16.140	13.358	15.460	13.358	14.007	21.778
L06	L*	42.356	50.875	50.875	41.925	42.356	35.538	37.967	42.356	35.538	53.400
	a*	7.159	6.983	3.667	7.159	7.159	5.667	7.159	1.200	3.667	5.500
	b*	16.140	21.778	14.100	14.007	16.140	13.358	17.292	13.358	13.358	21.778
L07	L*	40.329	50.875	50.875	35.538	42.356	35.538	37.967	40.329	40.329	53.400
	a*	7.159	7.159	3.667	7.159	5.667	7.159	7.159	1.200	3.667	5.500
	b*	14.007	19.900	14.100	13.358	16.140	13.358	17.292	14.007	14.007	21.778

**Analyses of Color Measurements using Illuminating Lamps**

The detailed CIELab color values obtained using different illuminating lamps used in the present study are provided in Table 3. Each table row represents L\*, a\* and b\* color values obtained using illuminating lamps (L01 to L07). On the other hand, each column represents the color values measured for each potato sample under test. The line plot for L\* color values obtained using the proposed methodology compared to standard L\* values for each potato sample is visualized in Fig. 5(a). L\* color values are displayed on the Y-axis of the line plot. In contrast, X-axis represents each potato sample under test. It can be identified that the line plot for the L01 lamp (illustrated in red color) nearly overlaps the line plot of standard L\* color values (represented in black color). Similarly, the line plot for L03 is also very close to the standard line plot; thus, L03 becomes the second-best lighting source to measure L\* color values of potato samples. On the other hand, line plots for the remaining lighting sources seem to be dispersed from the standard line plot. Thus, it can be identified that L01 is the best lighting source to measure potato samples' L\* color values.

Similarly, line plots for a\* color values obtained using the proposed methodology compared to standard a\* values for each potato sample are visualized in Fig. 5(b). It can be observed that line

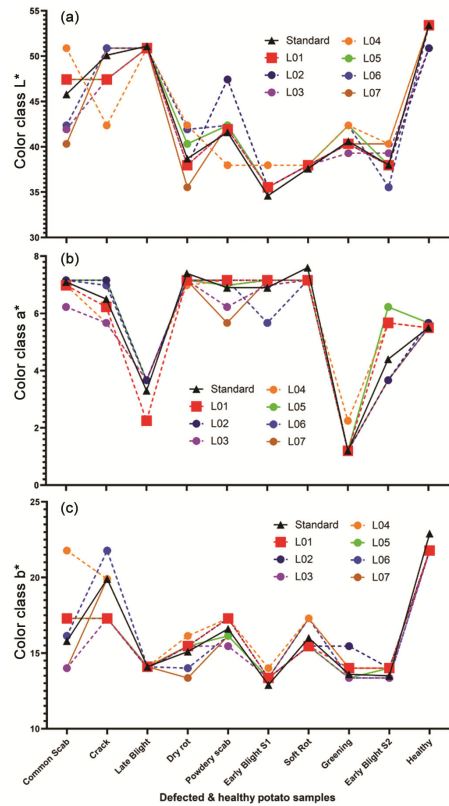


Fig. 5 — Line plot representing: (a) L\* color values obtained using proposed methodology compared to standard L\* values; (b) a\* color values obtained using proposed methodology compared to standard a\* values; (c) b\* color values obtained using proposed methodology compared to standard a\* values for each potato sample

Table 4 —  $\Delta E^*$  values obtained using each illuminating lamp (*L01 to L07*) for all potato samples

	$\Delta E^*$						
	L01	L02	L03	L04	L05	L06	L07
Common Scab	2.2093	2.2070	4.3584	7.8424	2.2070	3.4616	5.7580
Crack	3.7458	3.7933	3.8275	7.7891	3.7933	2.0881	1.0170
Late Blight	1.0700	0.4401	0.4401	0.4302	0.4302	0.4302	0.4302
Dry rot	0.8518	0.8518	0.8518	3.8234	1.6853	3.4137	3.6185
Powdery Scab	0.8073	5.8717	1.3641	3.7077	0.8885	0.9216	1.5177
Early Blight S1	1.0751	1.0751	1.0468	3.5535	1.0751	1.6155	1.0751
Soft Rot	0.7880	0.7880	0.7880	1.4140	0.7880	1.4140	1.4140
Greening	0.4893	1.8797	1.3223	2.0858	1.7722	1.7722	0.4893
Early Blight S2	1.3648	0.8922	1.8206	2.6989	1.8944	2.5733	2.4934
Healthy	1.1222	2.7682	2.7631	1.1222	1.1345	1.1222	1.1222
Average $\Delta E^*$	<b>1.3524</b>	2.0567	1.8583	3.4467	1.5669	1.8812	1.8935

plots for each lighting source are less dispersed from the standard plot when compared to the line plot for  $L^*$  color values in Fig. 5(a). This authorizes that  $a^*$  color values are less dependent on the lighting source used to capture color values of potato samples. After having a closer look, it can be identified that the line plot for  $a^*$  color values obtained using *L01* lighting source (represented in red color) is very close to the line plot obtained using standard  $a^*$  color values (represented in black color). Thus similar to  $L^*$  color values *L01* is the best lighting source to measure  $a^*$  color values for potato defect detection.

Identical results are obtained in a line plot for  $b^*$  color values visualized in Fig. 5(c). Similar to the previous results, the line plot for  $b^*$  color values obtained using the *L01* lighting (represented in red) sample nearly overlaps the standard line plot (illustrated in black). On the other hand  $b^*$  line plot obtained using the *L04* lighting source provides the worst results compared with standard  $b^*$  color values for potato samples.

#### Analyses of Color Difference $\Delta E^*$ Obtained using Illuminating Lamps (*L01–L07*)

When two colors are compared in CIELab space, the total color difference is calculated in terms of  $\Delta E^*$ . In the present study,  $\Delta E^*$  measures the color difference between the colors of potato samples measured under illuminating lamps (*L01 to L07*) and standard color values measured using an X-Rite Spectrocolorimeter. The  $\Delta E^*$  values obtained using each illuminating lamp used in the present study for all potato samples are elaborated in Table 4. Each row in the table except the last row provides  $\Delta E^*$  value obtained for different potato samples using lamps (*L01 to L07*). The last row of the table provides average  $\Delta E^*$  value obtained using each illuminating

lamp. The bold value corresponds to the lowest average  $\Delta E^*$  obtained when color was measured using different illuminating lamps. It can be observed that *L01* illuminating lamp obtained the lowest average  $\Delta E^*$  value and thus can be classified as the best illuminating lamp for measuring color in potato defect detection devices.

In Fig. 6(a)  $\Delta E^*$  violin plots of predicted color values using illuminating lamps (*L01 to L07*) are visualized. Color measuring accuracy under illuminating lamps (*L01 to L07*) is compared in terms of  $\Delta E^*$  using these plots. It is noteworthy that each violin contains a total of ten  $\Delta E^*$  values (i.e. one for each potato sample under study). The observations obtained are outlined below:

- In terms of the median  $\Delta E^*$  value in each violin, the overall deviation in color measuring accuracy among the seven illuminating lamps is significant for *L04* and *L06* lighting sources. It can be identified that the *L01* lighting source obtained the smallest median value for  $\Delta E^*$  and thus provides the best color-measuring accuracy for all potato samples.

- In terms of the “Third Quartile range”  $\Delta E^*$  value in each violin, *L01* provides the lowest  $\Delta E^*$  value since its “Third Quartile range” in violin is the lowest among compared illuminating lamps. Similarly, *L04* perform worst by achieving the highest  $\Delta E^*$  values since its “Third Quartile range” in its violin is highest among compared illuminating lamps.

- In terms of the “First Quartile range” in each violin, all illuminating lamps provide similar  $\Delta E^*$  values except for *L04* illuminating lamp. The *L04* provides the worst results since its “First Quartile range” in violin is the highest among compared lighting sources.

Experimental results obtained by implementing the proposed methodology to study the influence of

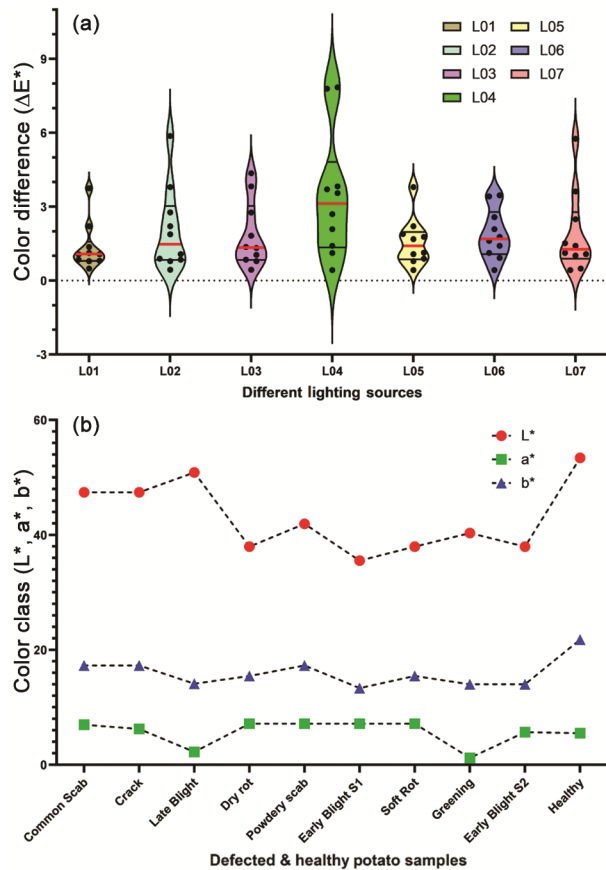


Fig. 6(a) — Violin plots representing  $\Delta E^*$  values obtained using illuminating lamps ( $L01$  to  $L07$ ); (b) Line plot representing values of all three CIELab color components for each potato sample using  $L01$  illuminating lamp

illuminating lamps on color-based potato defect detection authorize that lighting source  $L01$  generates the best color-measuring results and can be used effectively to measure color in potato defect detection devices.

#### Analyses of CIELab Color Values Provided by $L01$ Illuminating Lamp

Since experimental results prove that  $L01$  (Compact Fluorescent lamp 45W, 6500 CCT) illuminating lamp provides the best color measuring accuracy for potato samples with the lowest average  $\Delta E^*$  value. This section provides a graphical overview of  $L^*$ ,  $a^*$  and  $b^*$  values obtained for each potato sample when  $L01$  was used as an illuminating source. The line plot for values of all three CIELab color components for each potato sample using  $L01$  illuminating lamp are visualized in Fig. 6(b). It can be visually observed that the line plot for all three color components behaves linearly parallel to the x-axis of the line plot. This determines that the accuracy of

colour measuring was maintained for each potato sample when color was measured using  $L01$  illuminating lamp. The line plot illustrates that significant performance enhancement was provided by  $L01$  illuminating lamp in terms of color-measuring accuracy.

#### Conclusions

An analysis of potato skin color measuring accuracy using seven different illuminating lamps is performed in the present study. The proposed study succeeded in standardization of illuminating lamps used in machine learning-based potato defect detection devices. The potato color measuring accuracy using seven different types of illumination lamps ( $L01$  to  $L07$ ) was analysed. The experiments used ten potato samples with different defects, including one healthy potato. The experimental results have shown that the lowest  $\Delta E^*$  was obtained when a Compact Fluorescent lamp 45W, 6500 CCT ( $L01$ ) was used as an illuminating lamp for measuring the color of ten potato samples. It was concluded that different illuminating lamps strongly influenced the chromaticity coordinate  $L^*$  of the CIELab system. The experimental study shows that the perceptual lightness ( $L^*$ ) difference between defected and healthy potato skin was more prominent using lamps with higher CCT than lamps with lower CCT. More the difference in perceptual lightness of defected and healthy potato skin higher is the defect detection accuracy of computer vision systems. Thus the present study also concluded that illuminating lamps with higher CCT are most appropriate for computer vision-based potato defect detection devices. This study will help in enhancing the overall profits of the potato supply chain and related industries by delivering quality potato products to end users. There may be some possible limitations in this study as the research experiments were primarily performed in a controlled laboratory environment where external light distractions have been controlled, and due to lack of funding, the study was performed on the most commonly used illuminating lamps. Thus as a future work, the study can be extended to include real-time illuminating lamp analysis in industrial environments, and more illuminating lamps can be included in the analysis. The influence of illuminating lamps used in computer vision-based defect detection devices for food products like tomatoes, apples, etc., where skin determines the food quality, can also be analysed in future studies.



## Acknowledgements

The authors are grateful to the Department of Computer Science & Engineering, Punjabi University, Patiala (Pb.), India and the University Computer Centre (UCC), Punjabi University, Patiala (Pb.), India, for provisioning necessary facilities for successful execution of present work.

## References

- 1 Faostat, 2021, [<http://www.fao.org> (23 June 2023)]
- 2 Marino S, Beuseroy P & Smolarz A, Weakly-supervised learning approach for potato defects segmentation, *Eng Appl Artif Intell*, **85** (2019) 337–46. <https://doi.org/10.1016/j.engappai.2019.06.024>
- 3 Thenmozhi S, Lakshmi R J, Kumudavalli M V, Ibrahim I & Mohan R, A novel plant leaf ailment recognition method using image processing algorithms, *J Sci Ind Res*, **80(11)** (2021) 979–984.
- 4 Blasco J, Aleixos N, Gómez-Sanchis J & Moltó E, Recognition and classification of external skin damage in citrus fruits using multispectral data and morphological features, *Biosyst Eng*, **103(2)** (2009) 137–145.
- 5 Barnes M, Duckett T, Cielniak G, Stroud G & Harper G, Visual detection of blemishes in potatoes using minimalist boosted classifiers, *J Food Eng*, **98(3)** (2010) 339–346.
- 6 Razmjoooy N, Mousavi B S & Soleymani F, A real-time mathematical computer method for potato inspection using machine vision, *Comput Math with Appl*, **63(1)** (2012) 268–279.
- 7 ElMasry G, Cubero S, Moltó E & Blasco J, In-line sorting of irregular potatoes by using automated computer-based machine vision system, *J Food Eng*, **112(1)** (2012) 60–68.
- 8 Moallem P, Razmjoooy N & Mousavi B S. Robust potato color image segmentation using adaptive fuzzy inference system, *Iran J Fuzzy Syst*, **11(6)** (2014) 47–65.
- 9 Brahimi M, Boukhalfa K & Moussaoui A, Deep learning for tomato diseases: classification and symptoms visualization, *Appl Artif Intell*, **31(4)** (2017) 299–315.
- 10 Zhang S, Zhang S, Zhang C, Wang X & Shi Y, Cucumber leaf disease identification with global pooling dilated convolutional neural network, *Comput Electron Agric*, **162** (2019) 422–430.
- 11 Chauhan A & Singh M, Computer vision and machine learning based grape fruit cluster detection and yield estimation robot, *J Sci Ind Res*, **81(8)** (2022) 866–872.
- 12 Gomes J F S, Vieira R R, De Oliveira I A A & Leta F R, Influence of illumination on the characterization of banana ripening, *J Food Eng*, **120(1)** (2014) 215–222.
- 13 Oppenheim D & Shani G, Potato disease classification using convolution neural networks, *Adv Anim Biosci*, **8(2)** (2017) 244–249.
- 14 Su Q, Kondo N, Li M, Sun H, A I Riza D F & Habaragamuwa H, Potato quality grading based on machine vision and 3D shape analysis, *Comput Electron Agric*, **152** (2018) 261–268.
- 15 Ming W, Du J, Shen D, Zhang Z, Li X, Ma J R, Wang F & Ma J, Visual detection of sprouting in potatoes using ensemble-based classifier, *J Food Process Eng*, **41(3)** (2018) e12667, <https://doi.org/10.1111/jfpe.12667>.
- 16 Marino S, Beuseroy P & Smolarz A, Unsupervised adversarial deep domain adaptation method for potato defects classification, *Comput Electron Agric*, **174** (2020) 105501.
- 17 Si Y, Sankaran S, Knowles N R & Pavek M J, Image-based automated potato tuber shape evaluation, *J Food Meas Charact*, **12(2)** (2018) 702–709, <https://doi.org/10.1007/s11694-017-9683-2>.
- 18 Olkkonen M, Hansen T & Gegenfurtner K R, Color appearance of familiar objects: Effects of object shape, texture, and illumination changes, *J Vis*, **8(5)** (2008) 1-16. <https://doi.org/10.1167/8.5.13>.
- 19 Colorimetry, 3<sup>rd</sup> edition, [<https://cie.co.at/publications/colorimetry-3rd-edition> (24 June 2023)].
- 20 de Almeida T H, de Almeida D H, Gonçalves D & Lahr F A R, Color variations in CIELAB coordinates for softwoods and hardwoods under the influence of artificial and natural weathering, *J Build Eng*, **35** (2021) 101965.
- 21 Dobrzański B & Rybczynski R, Influence of packing method on colour perception improving the appearance of fruits and vegetables, *Res Agric Eng*, **54(2)** (2008) 97–103.
- 22 Wyszecki G & Stiles W S, *Color Science: concepts and methods, quantitative data and formulae* (John Wiley & Sons, New York) 2000, 968.
- 23 Kumar A & Choudhury R, Colour measurement instruments, in *Principles of colour and appearance measurement, 1<sup>st</sup> edn*, edited by A Kumar & R Choudhury (Woodhead Publishing, India) 2014, 221–269.
- 24 Hadimani L & Mittal N, Development of a computer vision system to estimate the colour indices of Kinnow mandarins, *J Food Sci Technol*, **56(4)** (2019) 2305–2311.
- 25 Breiman L, Random Forests, *Mach Learn*, **45(1)** (2001) 5–32. <https://doi.org/10.1023/A:1010933404324>.
- 26 Breiman L, Friedman J H, Olshen R A & Stone C J, *Classification and regression trees* (Routledge, New York) 1984, 1–358. <https://doi.org/10.1201/9781315139470>.
- 27 Loh W Y, Classification and regression trees, *Wiley Interdiscip Rev Data Min Knowl Discov*, **1(1)** (2011) 14–23.
- 28 Farhat N H, Support vector Regression, *IEEE Expert Syst Appl*, **7(5)** (1992) 63–72.
- 29 Zhang Z, Ding S & Sun Y, MBSVR: Multiple birth support vector regression, *Inf Sci*, **552** (2021) 65–79. DOI:10.1016/j.ins.2020.11.033.
- 30 Awad M & Khanna R, Support Vector Regression, in *Efficient Learning Machines: Theories, Concepts, and Applications for Engineers and System Designers*, Vol I, edited by M Awad & R Khanna (A press, Berkeley, CA) 2015, 67–80. [https://doi.org/10.1007/978-1-4302-5990-9\\_4](https://doi.org/10.1007/978-1-4302-5990-9_4).
- 31 Singh N & Singh P, Stacking-based multi-objective evolutionary ensemble framework for prediction of diabetes mellitus, *Biocybern Biomed Eng*, **40(1)** (2020) 1–22. <https://doi.org/10.1016/j.bbe.2019.10.001>.